Article

Silk Fiber Assembly Studied by Synchrotron Radiation SAXS/WAXS and Raman Spectroscopy

Anne Martel, Manfred Burghammer, Richard J. Davies,
Emanuela Di Cola, Charlotte Vendrely, and Christian Riekel

J. Am. Chem. Soc., **2008**, 130 (50), 17070-17074 • DOI: 10.1021/ja806654t • Publication Date (Web): 17 November 2008

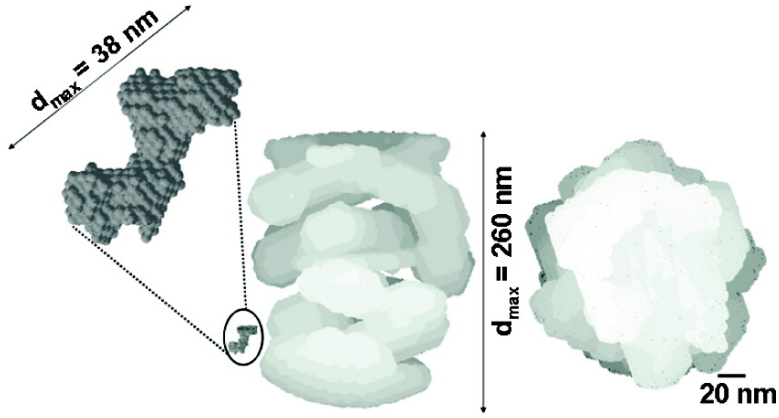

More About This Article

Additional resources and features associated with this article are available within the HTML version:

- Supporting Information
- Access to high resolution figures
- Links to articles and content related to this article
- Copyright permission to reproduce figures and/or text from this article

View the Full Text HTML

J|A|C|S
ARTICLES

Published on Web 11/17/2008

Silk Fiber Assembly Studied by Synchrotron Radiation SAXS/WAXS and Raman Spectroscopy

Anne Martel, Manfred Burghammer, Richard J. Davies, Emanuela Di Cola, Charlotte Vendrely, and Christian Riekel*

European Synchrotron Radiation Facility, B.P. 220, F-38043 Grenoble Cedex, France

Received August 27, 2008; E-mail: riekel@esrf.fr

Abstract: We have characterized the steps involved in silk assembly from the protein solution into β-type fibers by a combination of small-angle and wide-angle X-ray scattering and Raman spectroscopy. The aggregation process was studied in a concentric flow microfluidic cell, which allows mimicking the spinning duct. The fibroin molecule in solution shows an elongated shape with a maximum diameter of 38 nm. During the pH-driven initial assembly step, large-scale aggregates of fibroin molecules with a maximum diameter of about 260 nm are formed. Raman spectroscopy on the dried, fibrous material shows a principally α-helical silk I secondary structure, which is transformed gradually into β-type silk II by increasing immersion times in water. The formation of crystalline β-sheet domains within the fiber is confirmed by wide-angle X-ray scattering. The assembly process resembles the peptide condensation-ordering model proposed for amyloid cross-β formation.

Introduction

During silk spinning by silk worms and spiders, aqueous protein solution is converted into semicrystalline silk II fibers (called "filaments" or "threads"), which are essentially composed of β-sheet domains in a protein matrix.[1,2] X-ray and neutron small-angle scattering (SAXS/SANS) experiments on silk fibers provide evidence for a nanofibrillar morphology.[3−8] Shear forces induced on the aqueous protein (called "fibroin" for silkworms) dope by an elongational flow in the tapered spinning duct are assumed to play a key role in the β-transition.[9−11] Other contributing factors are the increase of the protein concentration along the spinning duct, a decrease in pH of the dope, and the presence of specific ions such as copper.[10,11]

Several assembly models have been proposed for the conversion of silk protein into a hierarchically organized β-type silk II fiber. In one model, native fibroin molecules are assumed to form directly β-sheet nuclei upon shearing with a subsequent β-sheet aggregation phase.[12] Rheo-SAXS in combination with Fourier transform infrared spectroscopy (FTIR)[13] and Rheo-NMR[14] of regenerated fibroin solution show, however, a more complex transformation with the formation of an amorphous intermediate with β-type conformation.[14] This material transforms upon drying into crystalline β-type silk II material with at least one further intermediate: a crystalline hydrated phase, attributed to silk I.[13] We note that crystalline hydrated silk I was also observed by wide-angle X-ray scattering (WAXS) in a study of the fibroin/H_2O/LiBr phase diagram.[15] The formation of silk II fibers in the spinning duct of silk worms and spiders is also thought to involve a silk I intermediate, which, according to different spectroscopic studies, consists mainly of β-turn[16] or conformations rich in α-helix.[17] Several silk I structures have been proposed on the basis of X-ray and electron diffraction data,[18−22] although their significance for the biospinning process has not been established. Circular dichroism (CD) and FTIR studies on model GA-rich peptides[17] suggest a transition from

(1) Fraser, R. D. B.; MacRae, T. P. *Conformations of Fibrous Proteins*; Academic Press: New York, 1973.
(2) Termonia, Y. *Macromolecules* **1994**, *27*, 7378–7381.
(3) Martel, A.; Burghammer, M.; Davies, R. J.; Riekel, C. *Biomacromolecules* **2007**, *8* (11), 3548–3556.
(4) Grubb, D. T.; Jelinski, L. W. *Macromolecules* **1997**, *30*, 2860–2867.
(5) Yang, Z.; Grubb, D. T.; Jelinski, L. W. *Macromolecules* **1997**, *30*, 8254–8261.
(6) Sapede, D.; Seydel, T.; Forsyth, T.; Koza, M. M.; Schweins, R.; Vollrath, F.; Riekel, C. *Macromolecules* **2005**, *38*, 8447–8453.
(7) Miller, L. D.; Putthanarat, S.; Eby, R. K.; Adams, W. W. *Int. J. Biol. Macromol.* **1999**, *24*, 159–165.
(8) Putthanarat, S.; Stribeck, N.; Fossey, S. A.; Eby, R. K.; Adams, W. W. *Polymer* **2000**, *41*, 7735–7747.
(9) Knight, D.; Knight, M.; Vollrath, F. *Int. J. Biol. Macromol.* **2000**, *27*, 205–210.
(10) Magoshi, J.; Magoshi, Y.; Nakamura, S. Mechanism of Fiber Formation of Silkworm, in Silk Polymers. In *Materials Science and Biotechnology*; Kaplan, D., Adams, W. W., Farmer, B., Viney, C., Eds.; Symposium Series 544; American Chemical Society: Washington, DC, 1994; pp 292−310.
(11) Vollrath, F.; Knight, D. P. *Nature* **2001**, *410*, 541–548.
(12) Li, G.; Zhou, P.; Shao, Z.; Xie, X.; Chen, X.; Wang, H.; Chunyu, L.; Yu, T. *Eur. J. Biochem.* **2001**, *268*, 6600–6606.
(13) Rössle, M.; Panine, P.; Urban, V. S.; Riekel, C. *Biopolymers* **2004**, *74*, 316–327.
(14) Ohgo, K.; Bagusat, F.; Asakura, T.; Scheler, U. *J. Am. Chem. Soc.* **2008**, *130*, 4182–4186.
(15) Sohn, S.; Strey, H. H.; Gido, S. P. *Biomacromolecules* **2004**, *5*, 751–757.
(16) Asakura, T.; Ashida, J.; Yamane, T.; Kameda, T.; Nakazawa, Y.; Ohgo, K.; Komatsu, K. A. *J. Mol. Biol.* **2001**, *396*, 291–305.
(17) Wilson, D.; Valluzzi, R.; Kaplan, D. *Biophys. J.* **2000**, *78*, 2690–2701.
(18) Lotz, B.; Keith, H. D. *J. Mol. Biol.* **1971**, *61*, 201–215.
(19) He, S. J.; Valluzzi, R.; Gido, S. P. *Int. J. Biol. Macromol.* **1999**, *24*, 187–195.
(20) Kratky, O.; Schauenstein, E.; Sekora, A. *Nature* **1950**, *165*, 319–320.
(21) Okuyama, K.; Somashekar, R.; Nogushi, K.; Ichimura, S. *Biopolymers* **2001**, *59*, 310–319.
(22) Lotz, B.; Cesari, F. C. *Biochimie* **1979**, *61*, 205–214.

10.1021/ja806654t CCC: $40.75

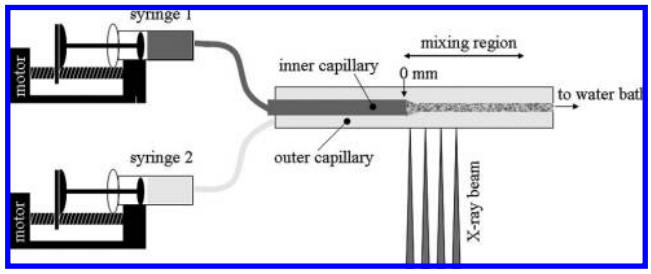

Figure 1. Tube-in-square-capillary microfluidic cell showing schematically the probing beam at four positions from the mixing point; motorized syringes are used to push the liquids into the capillaries.

a silk I structure rich in α-helix and random conformation to a silk II, which is rich in β-sheets. Another study on model peptides using the molecular dynamics simulation technique suggests that the silk I to silk II transition would rather consist of the folding of β-turns structures into β-sheets.[23]

The formation of fibroin micelles at the onset of fibroin assembly prior to the β-transition was deduced from optical and scanning electron microscopy (SEM) observations on aqueous fibroin/PEO blends.[24] Aggregates attributed to micellar morphologies have also been observed by optical microscopy during the assembly of artificial silk protein into a fiber in a lamellar flow microfluidic cell.[25] A microstructural characterization was, however, not performed. These results bear a similarity to amyloid fibril formation, which can be modeled as a competition between an initial condensation of polypeptide chains and their subsequent transformation into a cross-β structure.[26] We note in this context that the similarity of β-sheet silk assembly to cross β-sheet amyloid formation has already been pointed out.[27,28]

One can argue that progress in our understanding of silk assembly in nature requires more detailed microscopic studies under conditions close to biospinning. This is also the case for other β-sheet formation processes such as amyloid fibrillation.[26] We will show in this Article that the combination of structural (SAXS/WAXS) and spectroscopic (Raman) techniques provides novel information on the structural and conformational changes occurring during fibroin protein assembly. The use of a microfluidic cell allows mimicking the influence of various parameters on the assembly process. We have chosen to demonstrate this for the onset of assembly initiated by a pH jump of the fibroin solution. While not completely equivalent to the natural conditions, this setup is a further step toward mimicking the biospinning.

Results and Discussion

The fibroin molecule assembly process was studied in a microfluidic mixing cell with concentric geometry,[29] which allows mimicking the geometry of the silkworm spinning duct[10] (Figure 1). Details on the fibroin solution preparation and the microfluidic cell are reported in the Supporting Information.

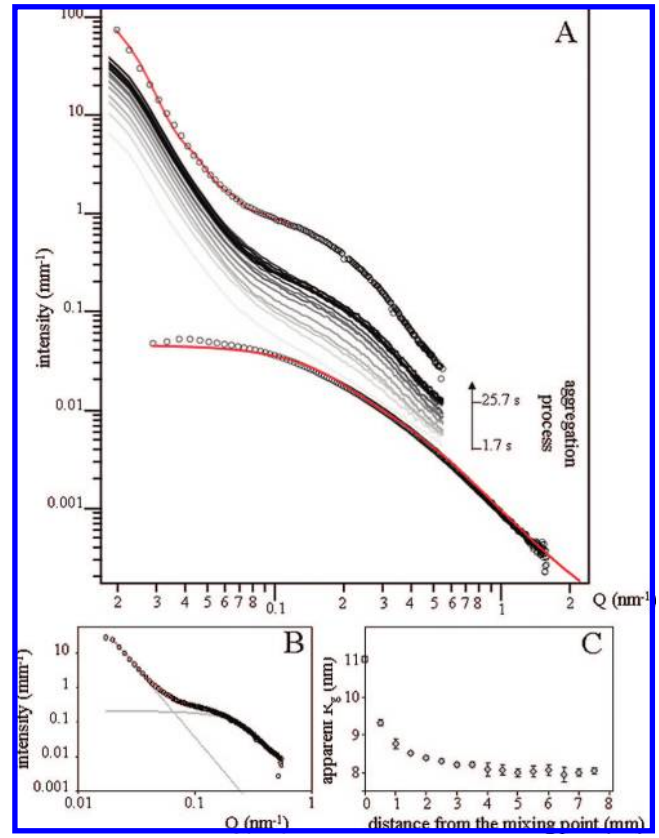

Figure 2. (A) Scattering curves of fibroin in solution (lowest circles curve), development of scattering along the aggregation zone (solid gray to black curves), and fully aggregated fibroin (upper circles curve). The curves have been shifted for clarity. The solid red curves show the model fits as discussed in the text (see the Supporting Information for the "DAMMIN" software). (B) Separation of the fully aggregated curve into two functions by the "unified scattering function"[31] ($Q = 4\pi \sin \Theta\lambda^{-1}$, where Θ is the Bragg scattering angle and λ is the wavelength). (C) Apparent radius of gyration (R_g) of fibroin molecule as a function of the distance from the inner capillary exit in the microfluidic cell. The first data point at the very exit (0 mm) corresponds to pure fibroin solution scattering analysis derived from flow-through capillary experiments.

We simulated the acidification step in natural fibroin assembly by injecting the fibroin solution in the inner tube and a pH 2 phosphate buffer in the outer tube of the microfluidic cell.[29] These conditions are still far away from the parameters of the biospinning (shear forces, higher fibroin concentration, higher pH, presence of other chemicals), but this setup is a step closer to mimicking the natural process of silk fiber formation as compared to the use of fibroin degraded by inadequate degumming protocol[29] or methanol to induce the silk I to silk II conversion.[30]

SAXS experiments on fibroin solutions and during fibroin aggregation were performed using synchrotron radiation at the European Synchrotron Radiation Facilities. Details on the instrumentation used, the data collection, and data analysis are reported in the Supporting Information. Figure 2A shows that the curve obtained immediately after mixing (light gray) is of composite nature and extends to smaller Q-values (larger objects) than does the pure fibroin scattering curve. The curves obtained after the mixing point have been separated into two

(23) Yamane, T.; Umemura, K.; Nakazawa, Y.; Asakura, T. *Macromolecules* **2003**, *36*, 6766–3772.
(24) Jin, H. J.; Kaplan, D. L. *Nature* **2003**, *424*, 1057–1061.
(25) Rammensee, S.; Slotta, U.; Scheibel, T.; Bausch, A. R. *Proc. Natl. Acad. Sci. U.S.A.* **2008**, *105*, 6590–6595.
(26) Auer, S.; Dobson, C. M.; Vendruscolo, M. *HFSP J.* **2007**, *1*, 137–146.
(27) Kenney, J. M.; Knight, D.; Wise, M. J.; Vollrath, F. *Eur. J. Biochem.* **2002**, *269*, 4159–4163.
(28) Slotta, U.; Hess, S.; Spiess, K.; Stromer, T.; Serpell, L.; Scheibel, T. *Macromol. Biosci.* **2007**, *7*, 183–188.
(29) Martel, A.; Burghammer, M.; Davies, R.; Di Cola, E.; Panine, P.; Salmon, J. B.; Riekel, C. *Biomicrofluidics* **2008**, *2*, 024104-1–024104-7.
(30) Chen, X.; Knight, D. P.; Shao, Z.; F, V. *Polymer* **2001**, 9969–9974.

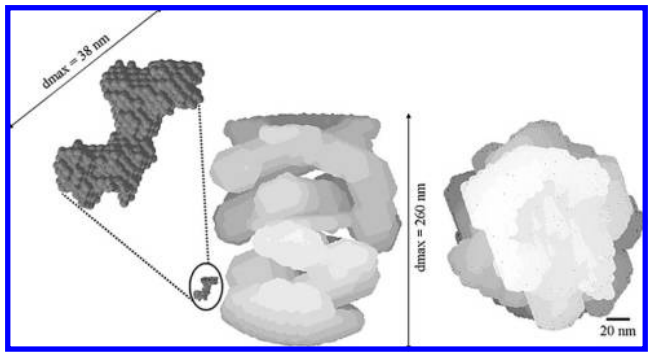

Figure 3. Left: Model for fibroin molecule derived from the average of 14 molecular shapes of a 5 mg/mL fibroin solution (see Supporting Information for the "DAMMIN" software). Right: Molecular shape of large aggregate in two different orientations. The size of the fibroin molecule is given for comparison.

components by using the "unified scattering function" approach (see Supporting Information)[31] (Figure 2B). We note for comparison that the radius of gyration of the native fibroin molecule in solution is $R_g = 10.8$ nm.[29] The fibroin molecule inside the aggregates has an apparent radius of gyration of about 8 nm (Figure 2C). The apparent radius of gyration along the observation line is interpreted as an average of those two R_g values weighted by the proportion of fibroin in aggregate or solution. The plot of the apparent radius of gyration of the fibroin molecules as a function of the distance from the mixing point reveals therefore the advance of the diffusion process (Figure 2C). At this structural level, the power-law exponent p (eq 2 in Supporting Information) decreases from -2 at the first point of measurement to -3 for the totally aggregated material, which confirms the fact that fibroin adopts a compacted shape inside the aggregate. The larger aggregate has an apparent R_g value of about 104 nm. This is a lower limit value, as the scattering curve does not reach the Guinier range. The polydispersity index determined from the unified scattering function is 3.47 (see Supporting Information).

The SAXS solution scattering curves can be used to obtain information on the molecular shapes. Three examples of the shapes of fibroin molecule and aggregate determined by the DAMMIN software from the same scattering curve are given in the Supporting Information. These shapes are not identical but share several features. The fact that several shapes fit the experimental data can be attributed to the flexibility of the protein and aggregates in solution. The existence of different types of aggregates is also possible. The averaged shape of the fibroin molecule in solution prior to aggregation shows an elongated protein (Figure 3). The largest distance inside the molecule is $d_{max} = 38$ nm (Figure 3). The shape of the aggregate, under the assumption of monodispersity, reveals a hollow structure with a largest distance of $d_{max} \approx 260$ nm (Figure 3). By calculating approximately the volume of this aggregate and the fibroin molecule, it appears that the aggregate would be formed of about 2500 fibroin protein molecules. It is interesting to note that a helical oligomeric aggregate with 1240 molecules has been deduced from SAXS solution scattering for the first step of insulin amyloid fibrillogenesis.[32] We note that the insulin helical oligomer ($d_{max} = 20$ nm) and the fibril repeating unit ($d_{max} = 70$ nm) are smaller than the fibroin and its aggregate. The proposed repeating unit of the fibril, made of three intertwining protofibrils,[32] bears, however, some resemblance to the current aggregate. We do not know, however, whether the fibroin aggregate corresponds also to a repeating unit of fibrillogenesis, as no information on the growing fibrils can be obtained from the SAXS solution scattering, due to lack of Q-resolution.

The aggregation process in the microfluidic cell results in the formation of protein fibers, which are collected in a water bath.[29] Fibers which are left for several hours in the water bath change their physical aspect and become whiter and less elastic. We studied the changes of crystallinity by WAXS, and the changes of protein conformation by Raman spectroscopy for fibers kept immersed in water for selected times up to 24 h. Instrumental details are reported in the Supporting Information. The WAXS pattern of a fiber dried immediately after threading shows a diffuse halo due to an amorphous structure (Figure 4A). Between 4 and 12 h of immersion in the water bath, two more narrow rings emerge from this diffuse halo, which are attributed to β-sheet crystalline domains as their d-spacings (0.44 nm/0.36 nm) correspond to the silk II structure.[1,3] This suggests an evolution of an amorphous structure toward a semicrystalline silk II structure. The powder texture suggests a random orientation of the crystalline domains in contrast to natural silk.[3] Post treatment by stretching of the nascent fiber is expected to induce a better orientation along the fiber axis.

Raman scattering provides complimentary information on local conformational changes, which cannot be deduced from the WAXS pattern (Figure 4B). Thus, the dried fibroin fibers collected from the water bath show principally silk I features. We observe a gradual conversion to silk II by increasing the immersion time of the fibers in water up to 24 h prior to drying (Figure 4B). This suggests that both the conformational and the structural transitions take place in the time range of a few hours.

Specific bands of the Raman spectra can be used to quantify the fibroin conformational transition (Figure 5A). The two bands at 1103 cm^{-1} and around 1083 cm^{-1} are attributed to secondary structural features involving alanine.[33,34] The disappearance of the 1103 cm^{-1} band and the emergence of the 1083 cm^{-1} band are thought to be due to an α-helical $\rightarrow$ β-sheet conformational transition of the poly-Ala-Gly regions.[33] The band at 1103 cm^{-1} has been proposed as a marker of the silk I structural intermediate.[35] We note that several conformations are proposed for the GA-rich regions in this intermediate such as β-turns[16] or α-helix+random coil,[17] which could be due to the existence of several possible conformations of fibroin, other than the predominantly β-sheet conformation present in the silk II structure. We assume in this work, in agreement with other studies, that the structure characterized by the 1103 cm^{-1} Raman band is due to the silk I intermediate, whereas the 1083 cm^{-1} band is a signature of the silk II structure.[36] The plot of the relative intensity of the 1083 cm^{-1} band as a function of the immersion time in the water bath is shown in Figure 5B. The results suggest that the silk I α-helix-rich conformation is maintained for up to 4 h in the water bath. For immersion times

(31) Beaucage, G. *J. Appl. Crystallogr.* **1995**, *28*, 717–728.
(32) Vestergaard, B.; Groenning, M.; Rössle, M.; Kastrup, J. S.; Weert, M. v. d.; Flink, J. M.; Frokjaer, S.; Gajhede, M.; Svergun, D. I. *PLoS Biol.* **2007**, *5*, 1089–1097.
(33) Monti, P.; Freddi, G.; Bertoluzza, A.; Kasai, N.; Tsukada, M. *J. Raman Spectrosc.* **1998**, *29*, 297–304.
(34) Taddei, P.; Monti, P. *Biopolymers* **2005**, *78*, 249–258.
(35) Monti, P.; Taddei, P.; Freddi, G.; Asakura, T.; Tsukada, M. *J. Raman Spectrosc.* **2001**, *32*, 103–107.
(36) Rousseau, M. E.; Lefèvre, T.; Beaulieu, L.; Asakura, T.; Pézolet, M. *Biomacromolecules* **2004**, *5*, 2247–2257.

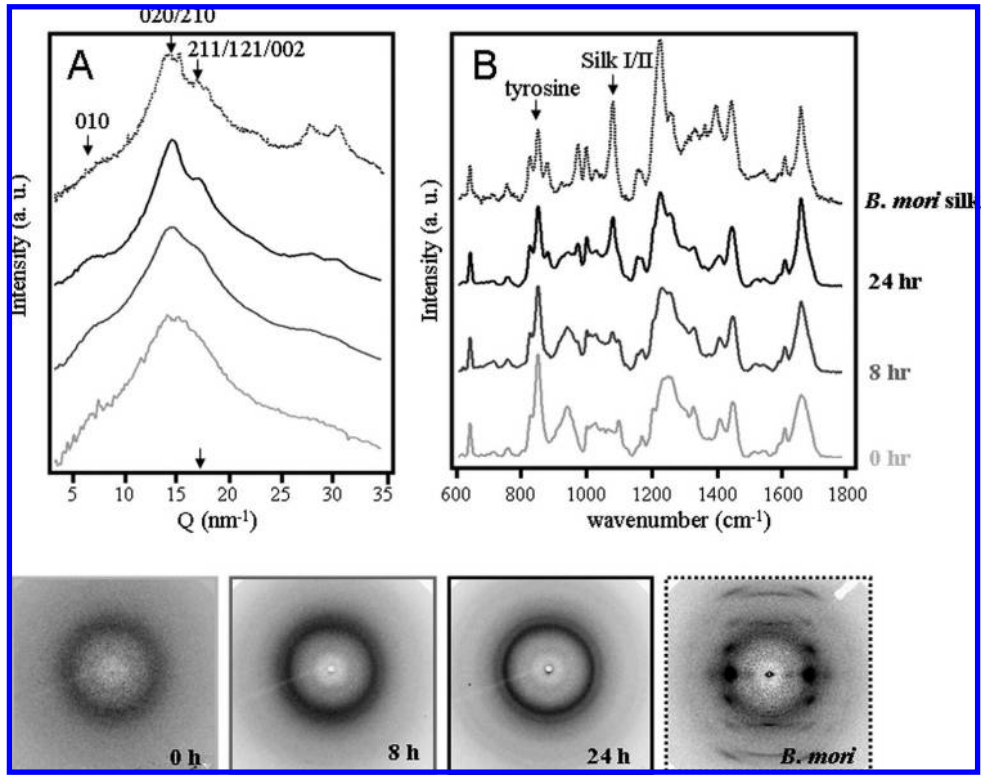

Figure 4. Influence on fibers of immersion time in water for (A) azimuthally regrouped WAXS patterns. The positions of selected reflections are indicated. The 2D-WAXS patterns are shown below.[3] (B) MicroRaman spectra; the spectral ranges sensitive to the tyrosine group environment and to the silk I/II transition are indicated. The fibers were dried prior to structural and spectroscopic studies.

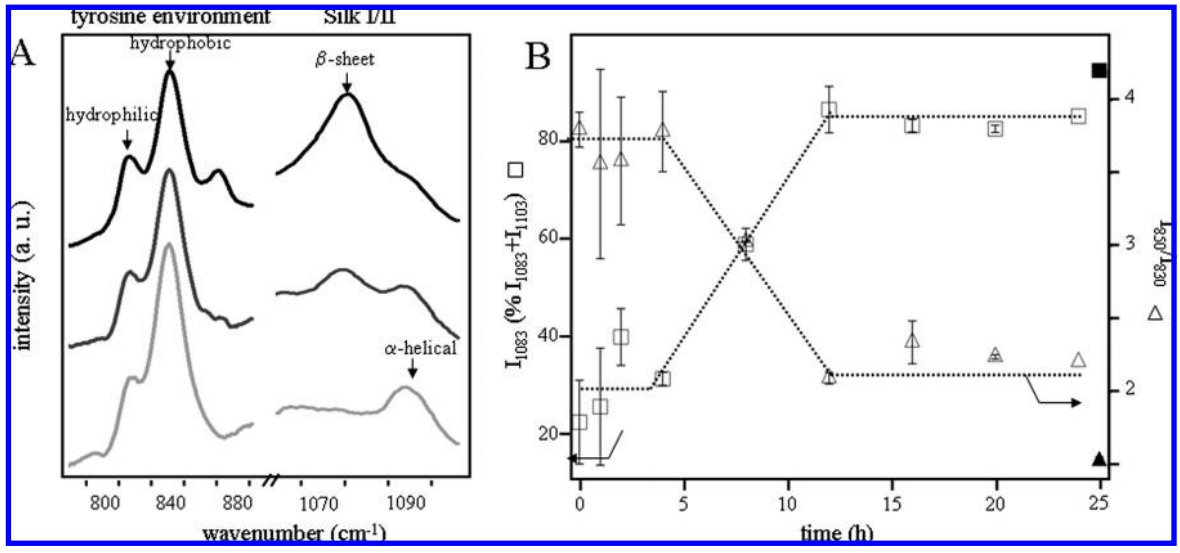

Figure 5. (A) Zoom on two zones of the Raman spectrum of the fiber dried immediately after spinning (light gray), after 8 h (dark gray), or 24 h (black) of immersion in water. The spectral assignments discussed in the text are indicated. (B) Silk I/II conversion determined from the 1100 cm^{-1} sensitive to the α-helical/β-sheet conformations (□) and for conversion from the 840 cm^{-1} zone sensitive to the tyrosine environment (△); the black symbols correspond to *Bombyx mori* silk. The lines are guides for the eye.

up to 12 h, the silk I/silk II conversion proceeds with the coexistence of the α-helix-rich silk I and the β-sheet-rich silk II. The structure does not evolve further up to 24 h.

The region around 830−850 cm^{-1} is sensitive to the tyrosines' environment. The changes observed in this region should be carefully interpreted, as each individual tyrosine could have a specific environment and the Raman spectrum shows an average of all these contributions.[37] Global information can, however, be derived from the ratio of the 850 cm^{-1} band intensity over the 830 cm^{-1} band intensity. A low I_{850}/I_{830} ratio suggests that the tyrosines groups are mostly buried in the protein and that the hydroxyl group of their side chain acts as a strong hydrogen-bond donor to an electronegative acceptor.[38] This is the situation observed in the natural silk Raman spectrum. A

(37) Siamwiza, M. N.; Lord, R. C.; Chen, M. C.; Takamatsu, T.; Harada, I.; Shimanouchi, H. M. *Biochemistry* **1975**, *14*, 4870–4876.

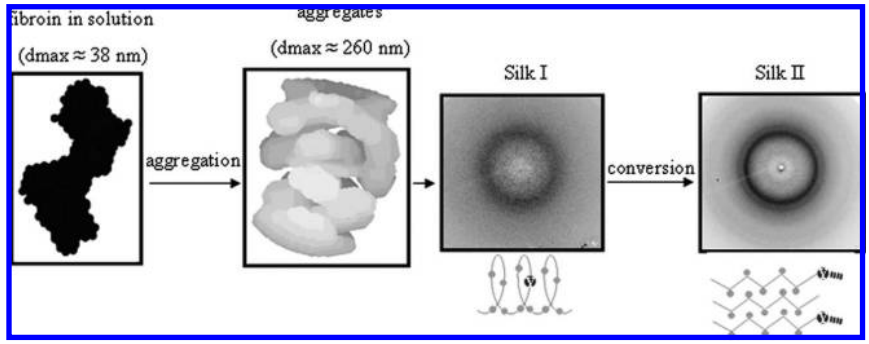

Figure 6. Schematic mechanism of fibroin assembly discussed in this article. Note that the silk I and silk II fibers' WAXS patterns were obtained after drying. The α-helical to β-sheet transformation of the glycine-alanine-rich regions is shown schematically with the global positions of the tyrosine groups.

very high I_{850}/I_{830} ratio, as in the regenerated silk I fiber spectrum, suggests that the tyrosines are mostly in a very hydrophobic environment.[34] The plot of the I_{850}/I_{830} ratio as a function of immersion time (Figure 5B) suggests that, during the silk I → silk II conversion, tyrosine groups change from a very hydrophobic environment to a more hydrophilic environment with which they form strong hydrogen bonds. As most of the tyrosine groups are situated in the GA-rich sequences, this change of environment can be correlated with the α-helical → β-sheet conformational transition.

Conclusions

Using the combination of microfluidics with X-ray scattering and Raman spectroscopy, we bring additional insights supporting the model of silk formation along two phases (aggregation of protein followed by the conversion from silk I to silk II) and details about this process (Figure 6). Under acidic conditions, the fibroin molecules aggregate into clusters having a radius of gyration larger than 100 nm and a maximum length of about 260 nm. The presence of this aggregate of defined shape discards the hypothesis of a fractal aggregation of fibroin. A similar structure has also been observed for insulin[32] and identified as a nucleus of amyloid fibrillogenesis. The existence of structure intermediary between this aggregate and the whole fiber is not excluded but could not be observed because of limitation in Q-resolution.

The formation of an amorphous aggregate prior to the β-transition resembles the condensation-ordering model proposed for amyloid formation at high peptide concentrations,[26] which passes through a step of aggregated molecules before reaching the β-sheet-rich conformation. The aggregate simulated shape does not resemble the spherical micelle model,[24] although it cannot be excluded that a hydrophilic/hydrophobic organization exists inside these aggregates. The micellar model[24] implies also a drastic change in protein shape in contrast to the current results, which show that the fibroin R_g changes only slightly upon aggregation. However, the time sequence proposed here, in which the aggregation takes place prior to the β-sheet folding, is compatible with the micellar hypothesis.

Once aggregated, the fibroin molecules exhibit predominantly random coil and helical conformation organized in a highly amorphous structure attributed to silk I. The conversion into the silk II structure implies that the glycine-alanine-rich blocks in the helices and unordered structures fold into β-sheets, which pleat into small crystalline domains. The tyrosine groups would move from a very hydrophobic to a more hydrophilic environment where they are involved in strong hydrogen bonds, probably linking the crystalline domains with the amorphous matrix. This model is in agreement with the observation on recombinant spider silk protein[25] resulting in the suggestion that the aggregation would be a prerequisite to the structural conversion into a β-sheet-rich fiber. Experimental evidence for larger-scale fibrillogenesis, as proposed for insulin amyloid fibrillogenesis,[32] would be expected from SAXS solution scattering at smaller Q-values and will require ultra small-angle X-ray scattering (USAXS).

The current model has to be used with care as it has been obtained under in vitro conditions. The natural spinning process is occurring for a more concentrated and viscous dope,[39,40] a more gradual pH decrease, and is influenced by other ions.[11] Moreover, the shear forces have not been mimicked in the present study, although they are thought to be important for silk formation in vivo.[11] Thus, in vitro Rheo-SAXS[13] and Rheo-NMR[14] show the formation of aggregates with β-type bonding. If shearing effects can be neglected, as in the present study, the silk I/silk II transformation apparently takes place more slowly, and an intermediary aggregate with α-helical bonding can be identified by Raman spectroscopy.

The present study provides a technical and conceptual basis to develop in vitro systems closer to the arthropod's spinning ducts, and to test sequentially the effect of the ions susceptible to be involved in the silk fiber formation process. The combination of structural and spectroscopic techniques could also be applied to amyloid formation to clarify the microstructure of aggregated material.[26]

Acknowledgment. We acknowledge gratefully a gift of *B. mori* cocoons by G. Freddi (Stazione Sperimentale per la Seta, Milano, Italy). We thank R. Gebhardt, T. Narayanan, M. Sztucki, B. Vestergaard, S. Hansen, and M. Rössle for help in SAXS data treatment as well as J. B. Salmon and the LOF (Pessac) for help with the development of the microfluidic cells. This work was supported by the EEC FP6 SAXIER grant.

Supporting Information Available: Fibroin protein structure and protein preparation, microfluidic cell, synchrotron radiation experiments, data analysis, and Raman spectroscopy. This material is available free of charge via the Internet at http://pubs.acs.org.

JA806654T

(38) Monti, P.; Freddi, G.; Sampaio, S.; Tsukada, M.; Taddei, P. *J. Mol. Struct.* **2005**, *744−747*, 685–690.
(39) Holland, C.; Terry, A. E.; Porter, D.; Vollrath, F. *Nat. Mater.* **2006**, *5*, 870–874.
(40) Terry, A. E.; Knight, D. P.; Porter, D.; Vollrath, F. *Biomacromolecules* **2004**, *5*, 768–772.